Nutrition and Cancer

ISSN: 0163-5581 (Print) 1532-7914 (Online) Journal homepage: www.tandfonline.com/journals/hnuc20

Andrographolide Exhibits Anticancer Potential Against Human Colon Cancer Cells by Inducing Cell Cycle Arrest and Programmed Cell Death via Augmentation of Intracellular Reactive Oxygen Species Level

Imran Khan, Fahad Khan, Arshi Farooqui & Irfan A. Ansari

To cite this article: Imran Khan, Fahad Khan, Arshi Farooqui & Irfan A. Ansari (2018) Andrographolide Exhibits Anticancer Potential Against Human Colon Cancer Cells by Inducing Cell Cycle Arrest and Programmed Cell Death via Augmentation of Intracellular Reactive Oxygen Species Level, Nutrition and Cancer, 70:5, 787-803, DOI: 10.1080/01635581.2018.1470649

To link to this article: https://doi.org/10.1080/01635581.2018.1470649

NUTRITION AND CANCER
2018, VOL. 70, NO. 5, 787–803
https://doi.org/10.1080/01635581.2018.1470649

Taylor & Francis
Taylor & Francis Group

Andrographolide Exhibits Anticancer Potential Against Human Colon Cancer Cells by Inducing Cell Cycle Arrest and Programmed Cell Death via Augmentation of Intracellular Reactive Oxygen Species Level

Imran Khan, Fahad Khan, Arshi Farooqui, and Irfan A. Ansari

Department of Biosciences, Integral University, Lucknow, India

ABSTRACT

Andrographolide, a diterpenoid lactone and a major constituent of *Andrographis paniculata* Nees, exhibits remarkable anticancer activity. However, the effect of andrographolide on colon cancer has not been completely elucidated yet. Thus, we investigated the chemopreventive potential of andrographolide in colon cancer HT-29 cells. The cytotoxic potential of andrographolide on HT-29 cells was determined by MTT assay, trypan blue exclusion assay, colony formation assay, and morphological analysis; and apoptotic property by DAPI and Hoechst staining, FITC-Annexin V assay, DNA fragmentation assay and caspase-3 activity assay. To elucidate andrographolide action, intracellular reactive oxygen species (ROS) level was determined by DCFDA dye; change in mitochondrial potential by Rhodamine123 and Mito Tracker Red CMXRos dye; and cell cycle modulatory property by flow cytometric analysis. Results of the study have shown that andrographolide decreased cell viability of HT-29 cells in a dose- and time-dependent manner. Furthermore, andrographolide induced apoptosis in HT-29 cells which seemed to be linked with augmented intracellular ROS level and disruption of mitochondrial membrane potential. Interestingly, andrographolide caused significant cell cycle arrest in G2/M phase at lower doses, but, in G0/G1 phase at higher doses. In summary, our results indicated that andrographolide exhibited antiproliferative and apoptotic properties against colon cancer HT-29 cells.

ARTICLE HISTORY
Received 5 July 2017
Accepted 22 February 2018

Introduction

Colorectal cancer, a frightening health problem, is the third most common cancer in males and second in females comprising 10% of all cancers (1,2). Globally, an estimated 1.4 million cases of colorectal cancer have been reported in 2012 with maximum occurrence rates in Northern America, Australia, New Zealand, Europe, and South Korea, and minimum in Africa and South Central Asia (2,3). The worldwide colorectal cancer-related fatalities are estimated to be approximately 693,000 in 2012, accounting for 8% of all cancer deaths and making colorectal cancer the fourth most common cause of death due to cancer (2). In India, colorectal cancer is the 10th most common cancer constituting 4% of cancer deaths (4). The annual incidence rates (AARs) for colon cancer in men and women are 4.4 and 3.9 per 100,000, respectively (4). In 2013, the highest AAR in men for colorectal cancer was recorded in Thiruvananthapuram (4.1) followed by Bangalore (3.9) and Mumbai (3.7). The highest AAR in women for colorectal cancer was recorded in Nagaland (5.2) followed by Aizwal (4.5) (4).

Despite recent advances, the prognosis of patients with advanced and metastatic colorectal cancer remains poor. Remedial options such as chemotherapy and radical colostomy are considered curative only for localized tumors and can restrain the metastasis and overcome recurrence (5). Nevertheless, drug resistance and side effects are still the major limitations to the chemotherapeutic use of these drugs (6). Currently, a great number of natural products have been found possessing anticarcinogenic property by counteracting different etiological factors (7).

Andrographis paniculata Nees (Family: Acanthaceae), known as Kalmegh or King of Bitters, is one of the most important medicinal plants extensively used in the traditional medicine of Southeast Asian countries (e.g., India and China) (8). *A. paniculata* is widely used in folk medicine as therapeutic lead for gastric and liver disorders, cold, influenza, and other infectious diseases (9). Extracts of the whole plant of *A. paniculata* have been reported to possess antioxidant, antibacterial, antifungal, anti-inflammatory, antidiabetic, anti-ulcerative, renal-protective, and cardio-protective properties (10,11). Its main

CONTACT Irfan A. Ansari, PhD iaansari@iul.ac.in Department of Biosciences, Integral University, Lucknow, Uttar Pradesh, India.
Color versions of one or more of the figures in the article can be found online at www.tandfonline.com/hnuc.

phytochemical andrographolide, a diterpenoid lactone, has been shown to have several pharmacological properties, including immunomodulatory, anti-inflammatory, and cytotoxicity actions (12,13). Recent studies have suggested a strong anticancer property of andrographolide which could be, therefore, applied as a potential chemopreventive agent (14). Andrographolide has been reported to induce cell cycle arrest and apoptosis, and inhibit tumor migration and invasion in different human cancer cell lines and models (15–17). Although, the role of andrographolide in the attenuation of colorectal cancer has begun to emerge with few preliminary reports, the mechanisms of the early events in the prevention of colorectal cancer formation have not yet been completely elucidated. Therefore, the aim of this study was to delineate the principal mechanism of action of andrographolide on colorectal cancer cell line HT-29.

Materials and Methods

Chemicals

Andrographolide, 2′,7′-dichlorodihydrofluorescein diacetate (DCFH-DA), Rhodamine123, DAPI (4′,6-diamidino-2-phenylindole), Hoechst 33342 (2′-(4-Ethoxyphenyl)-5-(4-methyl-1-piperazinyl)-2,5′-bi-1H-benzimidazole trihydrochloride), and propidium iodide (PI) solution were purchased from Sigma (St. Louis, MO, USA). Mito Tracker Red CMXRos was procured from Invitrogen. Dulbecco's modified eagle medium (DMEM), fetal bovine serum (FBS), crystal violet, 3-(4,5-dimethylthiazol-2-yl)-2,5-diphenyl tetrazolium bromide (MTT), and other chemicals were purchased from Himedia India, Ltd. (Mumbai, India). FITC Annexin V Apoptosis Detection Kit was obtained from BD Bioscience, PharMingen (San Diego, CA, USA). Caspase-3 Colorimetric Assay Kit was from BioVision, San Francisco, USA, and Apoptotic DNA ladder Kit was from G-Biosciences, Noida, India.

Cell Culture

Human colon cancer HT-29 and normal rat intestine epithelium IEC-6 cells were procured from National Centre for Cell Sciences (NCCS), Pune, India. Both were cultured in DMEM with 100 μg/ml penicillin/streptomycin/amphotericin B (Himedia, India, Ltd., Mumbai, India) and 10% heat-inactivated FBS. The cells were incubated at 37°C in a humidified atmosphere containing 5% CO_2.

Cell Viability Assay

The effect of andrographolide on HT-29 colon cancer cells was analyzed by MTT assay as described previously (18). Briefly, HT-29 cells (5×10^3 cells/well) were grown in a 96-well culture plate, allowed to adhere overnight, and further treated with different concentrations of andrographolide (1, 2, 4, 8, 16, 32, 64, 128, 256, 512, and 1024 μM) for 24 h. After that, 10 μl MTT (5 mg/ml) was added to each well and the plate was incubated for another 4 h at 37°C. Finally, 100 μl dimethyl sulfoxide (DMSO) was added to each well and the purple crystals were dissolved properly. The absorbance of each well was measured on a microplate reader (Bio-Rad, California, USA) at 490 nm and the cell survival was calculated as percentage (%) over the untreated control.

Trypan Blue Dye Exclusion Assay

Andrographolide-induced cytotoxicity in HT-29 cells was also determined by trypan blue exclusion assay, as described previously (19). Briefly, 5×10^4 cells were treated with or without andrographolide (1, 2, 4, 8, 16, 32, 64, 128, 256, 512 and 1024 μM) for 24 h, stained with 0.25% trypan blue dye and counted under a microscope using a hemocytometer. The result was expressed as the percentage of dead cells in each treatment group from three independent experiments.

Colony Formation Assay

The efficacy of andrographolide against HT-29 cells was tested using a colony formation assay (20). Briefly, approximately 4×10^2 cells were seeded in a 6-well plate tissue culture plates and treated with various concentrations of andrographolide (16, 32, 64, 128, and 256 μM) for 24 h. The cells were maintained under standard cell culture conditions at 37°C and 5% CO_2 in a humid environment. Colonies that formed in 1 week were fixed with chilled methanol, stained with 0.5% crystal violet, washed with water, and air-dried. Finally, photomicrograph was taken to analyze the effect of andrographolide on colony formation efficiency of HT-29 cells.

Morphological Analysis by Phase Contrast Microscopy

Morphological changes in the andrographolide-treated HT-29 cells were analyzed by a phase contrast microscope. The cells were grown overnight at a density of 5×10^3 cells per well in a 96-well plate and then re-supplemented with fresh medium having various concentrations of andrographolide (16, 32, 64, 128, and 256 μM); the cells were further incubated for 24 h under standard culture conditions. Finally, cellular morphology of untreated cells and treated cells were observed under inverted phase contrast microscope (Labomed, Los Angeles, USA).

Detection of Nuclear Condensation by DAPI Staining

Nuclear changes associated with andrographolide-treated HT-29 cells were also detected by DAPI staining. Briefly, HT-29 cells (5×10^4 cells/well) were grown in a 12-well plate for 24 h and then treated with various doses of andrographolide (16, 32, 64, 128, and 256 μM) for 12 h. After washing with cold phosphate buffer saline (PBS), cells were fixed in chilled methanol for 10 min. Subsequently, cells were permeabilized with permeabilizing buffer (0.25% Triton X-100) and stained with DAPI. Finally, cells were examined under an inverted fluorescence microscope (Nikon ECLIPSE Ti-S, Tokyo, Japan).

In addition, the nuclear morphological changes in HT-29 cells upon andrographolide treatment were further confirmed by using Hoechst 33342. Briefly, HT-29 cells (5×10^4 cells/well) were grown in a 12-well plate for 24 h and then treated with various doses of andrographolide (16, 32, 64, 128, and 256 μM) for 12 h. After washing with cold PBS, cells were stained with Hoechst 33342. Finally, cells were examined under an inverted fluorescence microscope (Nikon ECLIPSE Ti-S, Japan).

DNA Fragmentation Assay

DNA fragmentation assay was performed using G Bioscience apoptotic DNA ladder kit. Breifly, HT-29 cells (5×10^4 cells/well) were treated with andrographolide (16, 32, 64, 128, and 256 μM) for 24 h. Then, treated and untreated cells were collected by centrifugation, and DNA was extracted following the manufacturers protocol. The DNA fragmentation pattern was analyzed by electrophoresis on a 2.0% agarose gel.

FITC-Annexin V Assay to Analyze Apoptosis

Apoptosis in HT-29 cells was analyzed using the FITC-Annexin V/PI apoptosis kit (BD Biosciences, San Diego, CA, USA) according to the manufacturer's recommendations. Briefly, HT-29 cells were first seeded into 60-mm culture dishes and treated with andrographolide (16, 32, 64, 128, and 256 μM) for 24 h. The cells were washed twice with cold PBS and then resuspended in 1X binding buffer at a concentration of 1×10^6 cells/ml. Hundred microliters of the cell suspension (1×10^5 cells) was transferred to a 5-ml culture tube. Then, 5 μl of FITC-Annexin V conjugate and 5 μl PI were added to the cell suspension. After incubation for 15 min in the dark at room temperature (25°C), 400 μL of the 1X binding buffer was added to the cell suspension. The stained cells were then immediately analyzed on a FACS Calibur flow cytometer (BD Biosciences, San Diego, CA, USA).

Analysis of Caspase-3 Activity

The caspase-3 activity was determined by Caspase-3 Colorimetric Assay Kit (BioVision, USA). Briefly, 3×10^6 HT-29 cells untreated and treated with andrographolide (16, 32, 64, 128, and 256 μM) were lysed in 50 μl of chilled cell lysis buffer and incubated on ice for 10 min. The cell lysate was centrifuged for 1 min at 10,000 $\times$ *g* and the supernatant of the cell lysate was collected, and put on ice for instant assay. The cell lysate was properly diluted with 50 μl cell lysis buffer after protein quantification. Then, the lysate (50 μl) was aliquoted into a 96-well plate with 50 μl of reaction buffer, containing 10 mM DTT. After that, 5 μl of the 4-mM DEVD-pNA substrate was added in each well and incubated at 37°C for 1 h. Absorbance was then read at 405 nm in a microtiter plate reader. Percent (%) increase in caspase-3 activity was determined by comparing the result with the level of the uninduced control.

Analysis of the Effect of Caspase-3 Inhibitor (Z-DEVD-FMK)

To characterize the cytotoxicity of andrographolide, HT-29 cells were pretreated with 50 μM of Z-DEVD-FMK (a caspase-3 inhibitor) for 2 h and then treated with andrographolide at the indicated concentrations for 24 h. The cell viability was determined using the MTT assay as described above.

Measurement of Intracellular Reactive Oxygen Species (ROS) Level

The intracellular ROS generation was analyzed by DCFH-DA method. It is based on the ROS-induced formation of the highly fluorescent product 2′,7′-dichlorofluorescein (DCF) from the non-fluorescent dye 2′,7′-dichlorofluorescin diacetate (DCFH-DA). Briefly, HT-29 cells (5×10^4 cells per well) were grown in a 12-well plate for 24 h at 37°C. Subsequent treatment with andrographolide (16, 32, 64, 128, and 256 μM) for 12 h, cells were incubated with 10 μM DCFH-DA for 30 min at 37°C. Excessive DCFH-DA was removed by washing and images were captured by a fluorescence microscope (Nikon ECLIPSE Ti-S, Japan).

For the quantitative measurement of ROS production, HT-29 cells (1×10^4 per well) were grown in a 96-well black bottom culture plate for 24 h at 37°C. Then, the cells were treated with different doses of andrographolide as said above for 12 h, and further incubated with DCFH-DA (10 μM) for 30 min at 37°C. Fluorescence intensity was measured by multiwall microplate reader (Synergy H1 Hybrid Multi-Mode Microplate Reader,

BioTek, Santa Clara, USA) at excitation wavelength of 485 nm and emission wavelength of 528 nm. Data are expressed as the percentage of fluorescence intensity relative to control.

Analysis of the Effect of a ROS Inhibitor, N-Acetyl-L-Cysteine (NAC)

To affirm the generation of intracellular ROS in andrographolide-treated colon cancer cells, HT-29 cells were treated with 10 mM NAC for 2 h prior to andrographolide (16, 32, 64, 128, and 256 μM) for 12 h. After washing with PBS, cells were stained with 10 μM DCFH-DA for 30 min at 37°C. Fluorescence intensity was measured by multiwall microplate reader (Synergy H1 Hybrid Multi-Mode Microplate Reader, BioTek, USA) at excitation wavelength of 485 nm and emission wavelength of 528 nm. To further probe the role of excessive ROS generation in andrographolide-induced apoptosis in colon cancer cells, we examined the effect of andrographolide on HT-29 cells, pretreated with NAC (10 mM), by MTT assay.

Detection of the Mitochondrial Membrane Potential ($\Delta\Psi m$)

Alteration in the mitochondrial transmembrane potential in andrographolide-treated HT-29 cells was determined by rhodamine 123 (Rh123) staining. Briefly, HT-29 cells (2×10^5 cells/well) were grown in a 12-well plate and allowed to adhere overnight. Then, cells were co-cultured with different doses (16, 32, 64, 128, and 256 μM) of andrographolide for 12 h. Cells were washed and then stained with Rh123 (5 μg/ml) for 30 min in the dark. Finally, images were captured using an inverted fluorescence microscope (Nikon ECLIPSE Ti-S, Japan). In addition, Mito Tracker Red CMX Ros (Invitrogen), a selective mitochondrial fluorescent dye was also used to detect the alteration in mitochondrial potential. Briefly, HT-29 cells (2×10^5 cells/well) were grown in a 12-well plate and allowed to adhere overnight. Then, cells were co-cultured with different doses (16, 32, 64, 128, and 256 μM) of andrographolide for 12 h. Cells were washed and fixed with 3.5% paraformaldehyde for 15 min at 37°C and then permiabilized with 0.05% v/v Triton X-100. Finally, the cell were stained with Mito Tracker Red (25 ng/ml) for 30 min in the dark and images were captured using an inverted fluorescence microscope (Nikon ECLIPSE Ti-S, Japan).

Cell Cycle Analysis

The cell cycle phase distribution of andrographolide treated HT-29 cells was analyzed with PI as described earlier (21). Briefly, HT-29 cells (5×10^5 cells) were grown in a 60-mm tissue culture dish in the presence of 5% CO_2 for 24 h at 37°C and then treated with andrographolide (16, 32, 64, 128, and 256 μM) for another 24 h. Cells were collected, washed with PBS by centrifugation at 600 × g for 5 min and treated with RNase A (200 μg/ml) for 30 min at 37°C. Subsequently, cells were fixed with ice cold 70% ethanol and kept overnight at −20°C, and finally, stained with PI (25 μg/ml) for 15 min at room temperature. The cell cycle phase analysis was performed using a flow cytometer (Becton Dickinson FACS-Calibur, San Jose, CA, USA).

Statistical Analysis

The data shown in the study were the mean ± SEM of three independent experiments performed in triplicates. Statistical analysis was performed by one-way ANOVA using Dunnett's multiple comparison test and also by two-tailed, paired Student's t-test ($^{*}P<0.01$, $^{**}P < 0.001$, $^{***}P < 0.0001$ represent significant difference compared with control).

Results

Andrographolide did not Exert Significant Effect on Normal Colon Epithelial IEC-6 Cells

Initially, we evaluated the cytotoxic effect of andrographolide on normal colon epithelial IEC-6 cells by MTT assay. Results demonstrated that andrographolide did not impart significant inhibitory effect on normal colon epithelial cells. The data showed that after 24 h of treatment, percent viability of normal cells as compared to control was around 98.14%, 98.07%, 97.78%, 97.12% 96.21%, 95.22%, 94.31%, 94.78%, and 93.54% at 1, 2, 4, 8, 16, 32, 64, 128, and 256 μM dose of andrographolide, respectively; which were found to be statistically insignificant (Fig. 1A). Similarly, we did not find any significant effect on cell viability of colon epithelial cells after 48 h of andrographolide treatment with 1, 2, 4, 8, 16, 32, 64, 128, and 256 μM concentrations (Fig. 1A). Thus, cell viability assay demonstrated that doses 1, 2, 4, 8, 16, 32, 64, 128, and 256 μM of andrographolide did not show significant effect on cell viability on compared to control. However, a significant reduction in cell viability (90.56% and 89.34%) was observed at 512 and 1024 μM of andrographolide after 24 h of treatment (Fig. 1A). Similarly, cell viability was found to be substantially reduced to around 89.02% and 87.82% at 512 and 1024 μM of andrographolide after 48 h of treatment. Thus, the results showed that

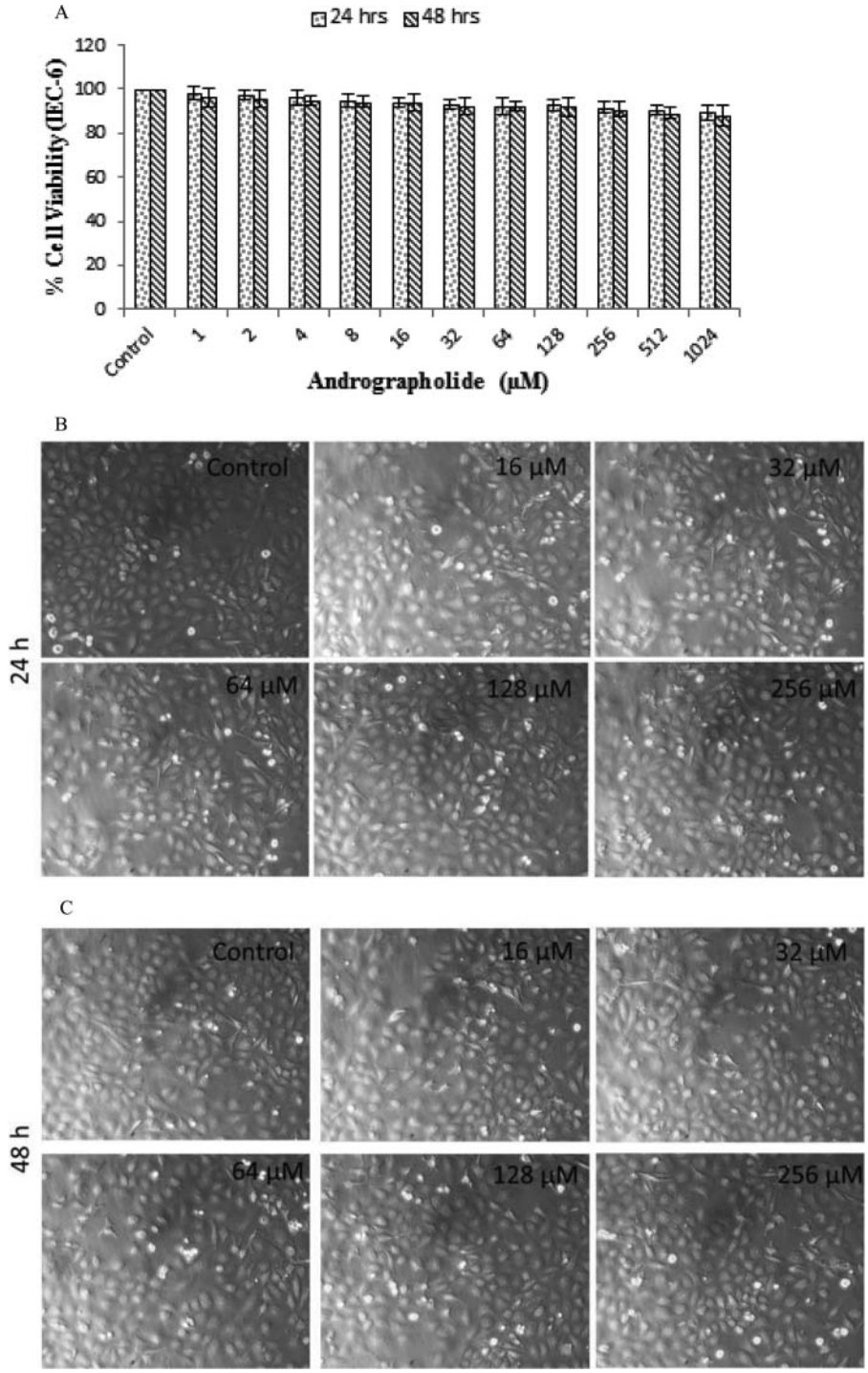

Figure 1. In vitro activity of andrographolide against normal colon epithelium IEC-6 cells. A: Insignificant effect of andrographolide on cell viability of normal IEC-6 cells treated with different doses of andrographolide (1–1024 μM) for 24 and 48 h assessed by MTT assay The results represented are the mean $\pm$ SEM of three independent experiments performed in triplicate ($^{*}P < 0.01$, $^{**}P < 0.001$ represent significant difference compared with control). B: Phase-contrast photomicrograph of IEC-6 cells treated with either vehicle control or different doses of andrographolide (16–256 μM) for 24 and C: 48 h. Images shown are representative of three independent experiments.

andrographolide exhibited considerable cytotoxicity in IEC-6 cells only at higher concentrations, i.e., 512 and 1024 μM (Fig. 1A). Furthermore, morphological study by phase contrast microscope suggested that after 24 and 48 h of treatment, higher concentrations of andrographolide (512 and 1024 μM) altered cell morphology and induced cell death in normal colon cells. However, dose of 1, 2, 4, 8, 16, 32, 64, 128, and

256 μM andrographolide, at above mentioned time periods, did not exert significant effect on cell morphology as revealed in Fig. 1B & C. Thus, the results of this study have established that andrographolide did not show considerable cytotoxic effect in normal colon epithelial cells.

Andrographolide Decreased Cell Viability and Induced Cytotoxic Effect in Human Colon Cancer HT-29 Cell Line

Subsequently, we tested the cytotoxic potential of andrographolide on human colon cancer HT-29 cell line by MTT assay. The cells were treated with varying concentration of andrographolide (1, 2, 4, 8, 16, 32, 64, 128, 256, 512, and 1024 μM) for 24 and 48 h. The treatment of HT-29 cells with andrographolide resulted in a significant decrease in cell viability as compared to controls. Andrographolide inhibited proliferation of HT-29 cells in a concentration- and time-dependent manner with minimum inhibitory concentrations (IC_{50}) of around 59.8 μM and 33.63 μM, for 24 h and 48 h, respectively (Fig. 2A). The results showed that after 24 h of treatment at 1, 2, 4, 8, 16, 32, 64, 128, and 256 μM of andrographolide, cell viability of HT-29 cells significantly reduced to around 78.22%, 74.43%, 68.13%, 62.53%, 56.32%, 51.78%, 49.87%, 46.99%, and 38.35%, respectively, as compared to control, which further dropped to 37.42% and 34.56% at 512 and 1024 μM, respectively. Similarly, after 48 h of treatment at 1, 2, 4, 8, 16, 32, 64, 128, 256, 512, and 1024 μM of andrographolide, viability of HT-29 cells reduced to around 76.55%, 67.13%, 65.83%, 58.17%, 55.04%, 50.84%, 48.09%, 43.23%, 36.87%, 35.72%, and 32.96%, respectively, as compared to control (Fig. 2A).

To support the findings of MTT assay, we evaluated the cytotoxic effect of andrographolide on the cell viability of HT-29 cells by trypan blue exclusion assay. Treatment of HT-29 cells with andrographolide, at the doses of 1, 2, 4, 8, 16, 32, 64, 128, 256, 512, and 1024 μM for 24 and 48 h, resulted in significant cell death (Fig. 2B). The results showed that when compared to control, treatment of HT-29 cells with andrographolide for 24 h resulted in significant amount of cell death of around 21.79%, 26.91%, 33.23%, 36.14%, 44.04%, 46.22%, 48.79%, 55.34%, 63.65%, 66.24%, and 68.12% at 1, 2, 4, 8, 16, 32, 64, 128, 256, 512, and 1024 μM, respectively; which further increased to around 23.88%, 28.88%, 35.14%, 40.24%, 46.97%, 49.52%, 50.91%, 57.44%, 66.46%, 69.29%, and 71.04% after 48 h of treatment at above mentioned doses (Fig. 2B). Thus, the above results have established that andrographolide could induce substantial cytotoxic effects on human colon cancer cells without incurring significant cytotoxic effect on normal colon epithelial cells.

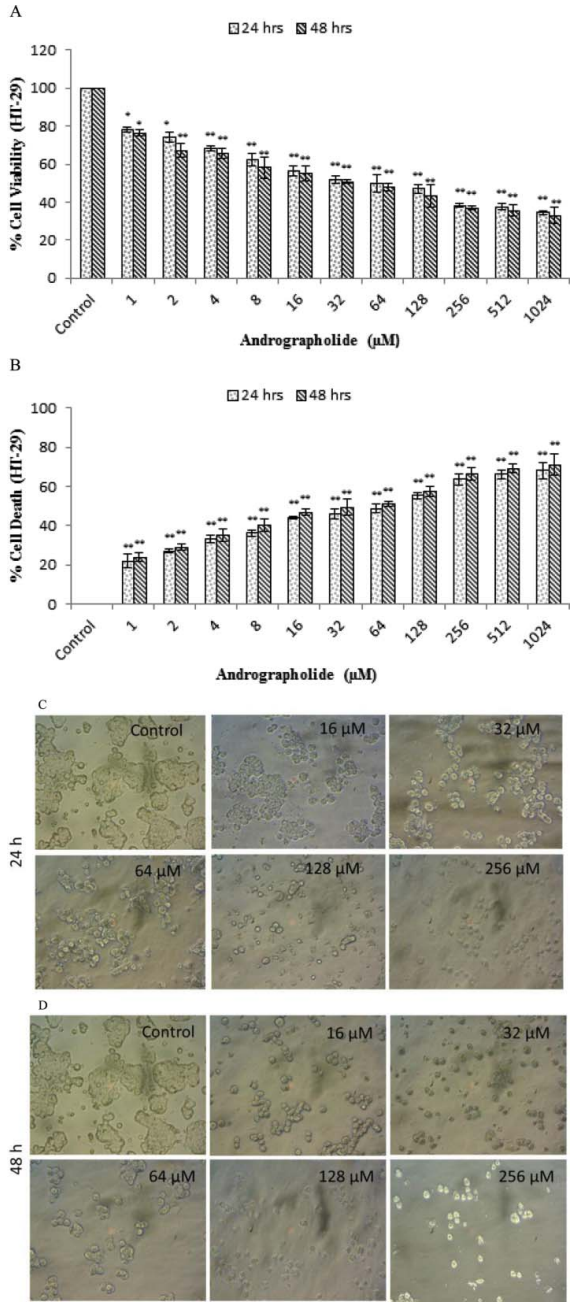

Figure 2. In vitro activity of andrographolide against colon cancer HT-29 cells. A: Percent cell viability of HT-29 cells treated with different doses of andrographolide (1–1024 μM) for 24 and 48 h assessed by MTT assay. B: Percent cell death of HT-29 cells treated with different doses of andrographolide (1–1024 μM) for 24 and 48 h assessed by trypan blue dye exclusion assay. The results represented are the mean ± SEM of three independent experiments performed in triplicate ($^{*}P < 0.01$, $^{**}P < 0.001$ represent significant difference compared with control). C: Phase-contrast photomicrograph of HT-29 cells treated with either vehicle control or different doses of andrographolide (16–256 μM) for 24 and D: 48 h. Images shown are representative of three independent experiments.

Andrographolide Induced Morphological Changes in HT-29 Cells

The cellular morphology of HT-29 cells upon treatment of different concentrations of andrographolide was assessed using inverted phase contrast microscope. Photomicrographs clearly depicted the morphological changes in the treated cells as compared to the control (Fig. 2C). Notable shrinkage in cell membranes of treated cells accompanied with detachment of cells from the surface of culture plates (Fig. 2D). These morphological changes in HT-29 cells were more prominent with the increased dose of andrographolide. In contrast, the untreated control cells exhibited well spread flattened morphology. These results were in concordance with the above findings, and we selected five optimum doses of andrographolide (16, 32, 64, 128, and 256 μM) around IC_{50} for further study.

Andrographolide Inhibited Colony-Forming Efficiency of HT-29 Cells

Colon cancer HT-29 cell line is a colony-forming cell line which forms dense colonies of cells in form of patches. Thus, the effect of andrographolide on colony-forming efficiency of HT-29 cells was assessed by colony formation assay. The number of colonies reduced in a dose-dependent manner, as shown in Fig. 3. Results showed that andrographolide inhibited colony formation at concentration as low as 16 μM, whereas andrographolide, at the dose of 32, 64, 128, and 256 μM showed fewer colonies of HT-29 cells with significantly reduced number compared to the control.

Andrographolide Caused Nuclear Condensation in HT-29 Cells

To characterize whether andrographolide-mediated inhibition of cell viability in colon cancer cells was a result of induction of apoptosis, DAPI and Hoechst 33342 staining was performed in andrographolide-treated and andrographolide-untreated HT-29 cells. Marked nuclear changes were observed in colon cancer cells after treatment with andrographolide (16, 32, 64, 128, and 256 μM) for 24 h. Apoptotic cells were identified with the presence of condensed nucleus, fragmented DNA, and perinuclear apoptotic bodies upon treatment of andrographolide. As observed from photomicrograph, untreated control cells demonstrated normal nuclear morphology displaying uniform circular shape and no condensation of chromatin. In contrast, andrographolide induced nuclear changes in HT-29 cells in a dose-dependent manner as indicated by arrows (Fig. 4A). Similarly, Hoechst 33342 staining also showed dose-dependent prominent nuclear changes in andrographolide-treated cells (Fig. 4B). The results of DAPI and Hoechst 33342 staining substantiated the phenomenon of apoptosis induction in HT-29 cells following treatment of andrographolide.

Andrographolide-Induced Apoptosis in HT-29 Cells

To ascertain whether reduction in the cell viability of HT-29 cells induced by andrographolide was due to apoptosis, annexin V-FITC/PI flow cytometric analysis was performed. Apoptotic cells exhibit externalization of phosphatidylserine (PS) on the cell surface as an early marker of apoptosis (22). Thus externalization of PS in HT-29 cells, upon treatment of andrographolide (16, 32, 64, 128, and 256 μM) for 24 h, was confirmed by double staining with annexin V-FITC/PI. Untreated viable cells stained negative for both Annexin V-FITC and PI (Q1). Treated group of cells staining positive for Annexin V-FITC and negative for PI were categorized as early apoptotic (Q2), cells staining positive for both Annexin V-FITC and PI as late apoptotic

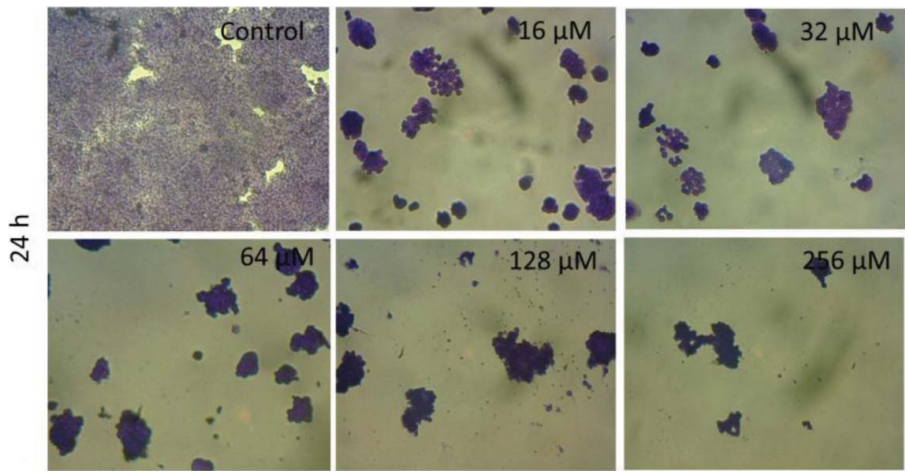

Figure 3. Colony formation assay. A: Phase-contrast photomicrograph of HT-29 cells treated with either vehicle control or different doses of andrographolide (16–256 μM) for 24 h. Images shown are representative of three independent experiments.

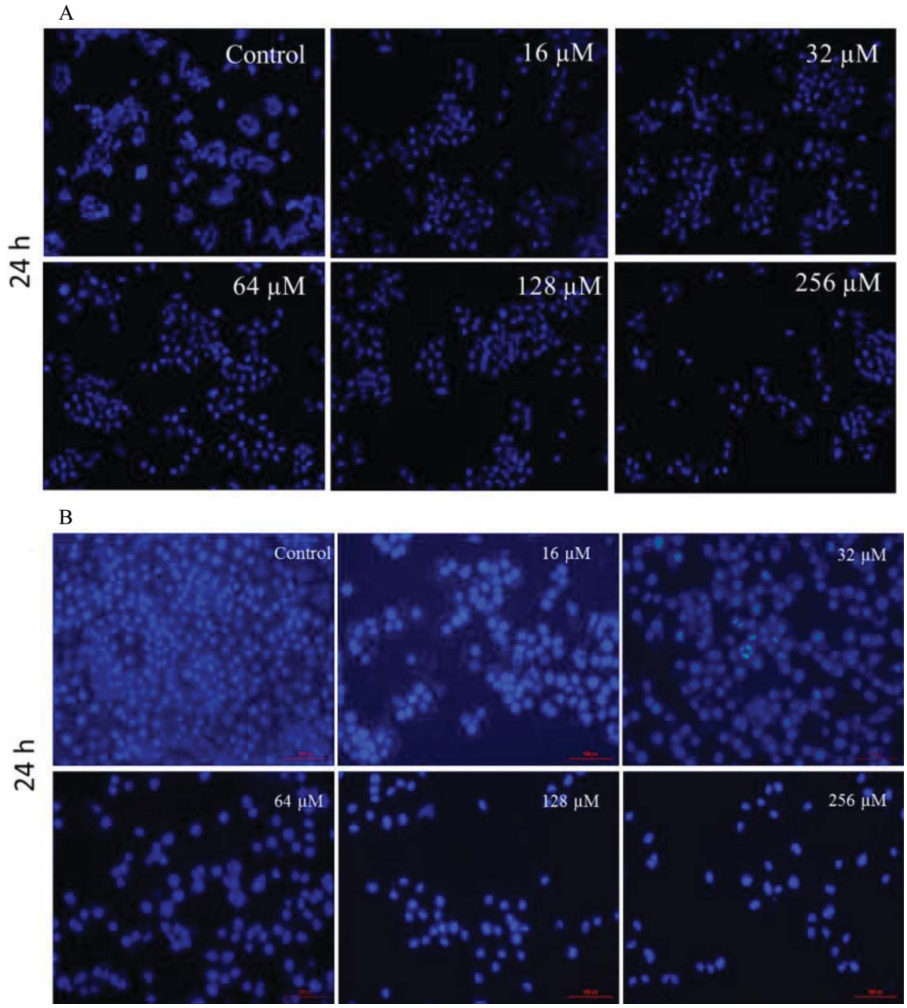

Figure 4. Andrographolide-induced nuclear condensation in human colon cancer HT-29 cells. Nuclear morphology of A: DAPI-stained and B: Hoechst-stained nuclei of HT-29 cells treated with varying concentrations of andrographolide (16–256 μM) for 24 h analyzed by fluorescence microscopy. Data shown are representative of three independent experiments. Images shown are representative of three independent experiments.

cells (Q3), and cells staining negative for Annexin V-FITC and positive for PI as dead or necrotic cells (Q4). As shown in Fig. 5A, the number of surviving cells reduced and the number of both early and late apoptotic cells increased in andrographolide-treated cells. The results showed that andrographolide induced significant amount of apoptosis in HT-29 cells of about 10.25%, 15.93%, 23.77%, 33.52%, and 43.09% after 24 h of treatment with 16, 32, 64, 128, and 256 μM of andrographolide, respectively (Fig. 5A & B). Thus, andrographolide induced apoptosis in HT-29 cells in a dose-dependent manner.

Andrographolide-Induced DNA Fragmentation in HT-29 Cells

DNA fragmentation is considered as one of the hallmarks of apoptosis; therefore, we investigated whether andrographolide treatment induces DNA fragmentation in colon cancer cells. Andrographolide (16, 32, 64, 128, and 256 μM) treatment in HT-29 cells for 24 h showed notable DNA fragmentation demonstrating a dose-dependent effect. Small shearing in DNA band was observed at 16 and 32 μM of andrographolide. However, dose of 64, 128, and 256 μM demonstrated relatively higher level of DNA fragmentation (Fig. 6).

Andrographolide-Induced Caspase Activation in Colon Cancer HT-29 Cells

Caspases are the cysteine-aspartate proteases which, upon conversion from pro to active forms, mediate the proteolytic cleavage of many key cellular proteins during apoptosis. Accordingly, we investigated whether andrographolide-induced apoptosis in HT-29 cells was due to the activation of caspases. Since caspase-3 is the main downstream effecter caspase in the

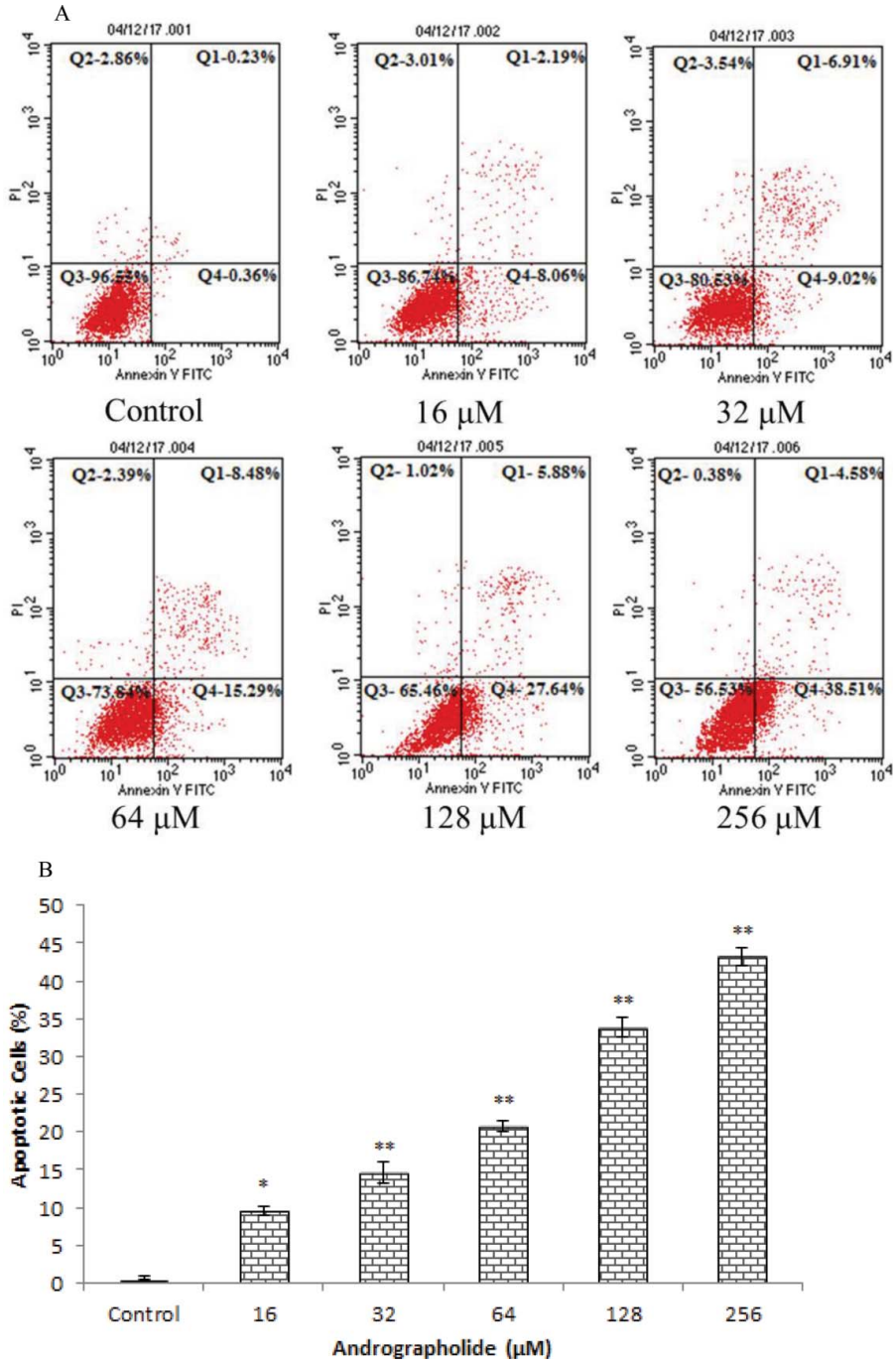

Figure 5. Andrographolide induced apoptosis in colon cancer HT-29 cells. A: Percent apoptosis in Annexin V-FITC/PI-stained HT-29 cells treated with varying concentrations of andrographolide (16–256 μM) for 24 h observed by flow cytometric analysis. The lower right (LR) quadrant of the histograms indicates the early apoptotic cells and the upper right (UR) quadrant indicates the late apoptotic cells. Data shown are representative of three independent experiments. B: Graphical representation of percent apoptosis as observed by Annexin V-FITC/PI assay. The results represented are the mean ± SEM of three independent experiments ($^{*}P < 0.01$, $^{**}P < 0.001$ represent significant difference compared with control).

apoptotic pathway, we determined its activity in andrographolide-treated and andrographolide-untreated control colon cancer cells. Our results showed a significant induction of caspase-3 activity in HT-29 cells after treatment with different doses of andrographolide for 24 h (Fig. 7A). Caspase-3 activity was drastically increased as compared to untreated control by around 39.26%, 55.95%, 82.54%, 103.79%, and 117.43% at the dose of 16, 32, 64, 128, and 256 μM of andrographolide, respectively (Fig. 7A). Thus, caspase-3 activity in andrographolide-treated HT-29 cells was found to be dose dependent.

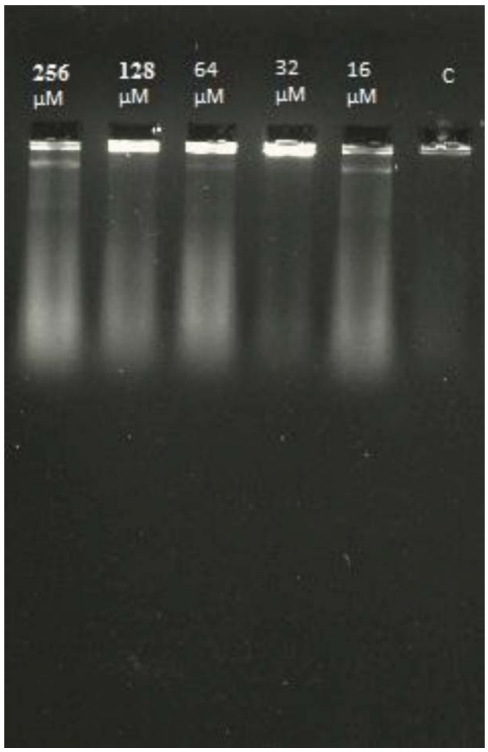

Figure 6. DNA fragmentation of HT-29 cells treated with andrographolide (16–256 μM) for 24 h observed by agarose gel electrophoresis.

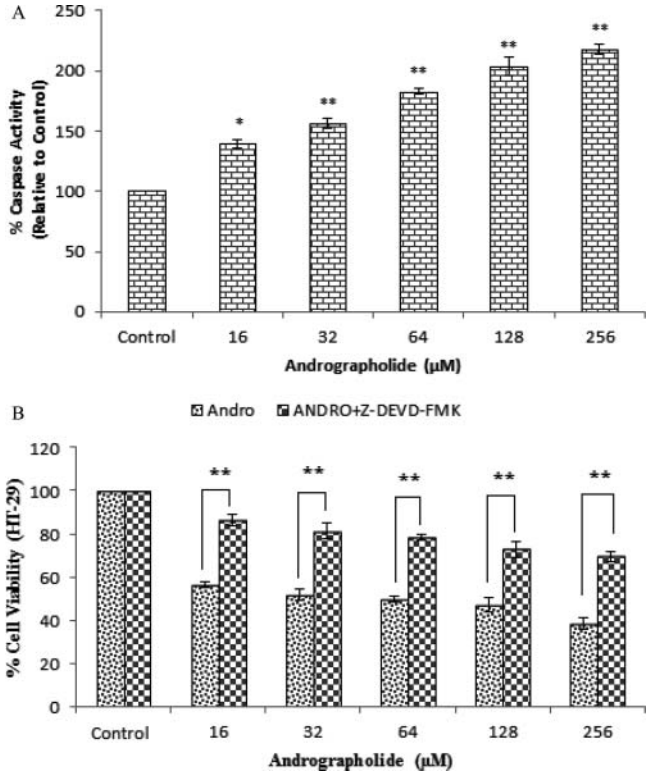

Figure 7. Activation of caspase-3 in andrographolide-treated HT-29 cells. A: Percent caspase-3 activity in HT-29 cells treated with different concentrations of andrographolide (16–256 μM) for 24 h. B: Percent cell viability of HT-29 cells pre-treated with a caspase-3 inhibitor, Z-DEVD-FMK followed by different doses of andrographolide (16–256 μM) for 24 h assessed by MTT assay. Data represent mean ± SEM of three independent experiments performed in triplicate ($^{*}P < 0.01$, $^{**}P < 0.001$ represent significant difference compared with control).

Attenuation of Andrographolide-Induced Apoptosis in HT-29 Cells by Caspase-3 Inhibitor

To further illustrate whether andrographolide-induced cytotoxicity in colon cancer cells was due to activation of caspase-3, the effect of andrographolide on colon cancer cells was determined by MTT assay in the presence of a caspase-3 inhibitor (Z-DEVD-FMK). Briefly, HT-29 cells were pretreated with 50 μM of Z-DEVD-FMK for 2 h followed by andrographolide (16, 32, 64, 128, and 256 μM) for an additional 24 h. The results showed that capase-3 inhibitor significantly reduced the amount of cytotoxicity in colon cancer cells induced by andrographolide (Fig. 7B). Thus, induction of caspase-3 activity played crucial role in andrographolide-induced apoptosis. However, pretreatment of Z-DEVD-FMK did not completely inhibit the cell viability in colon cancer cells which indicated the possible additional role of caspase-independent pathway of apoptosis also in andrographolide-treated HT-29 cells.

Andrographolide-Disrupted Mitochondrial Membrane Potential in HT-29 Cells

Disruption of the mitochondrial membrane followed by the loss in the $\Delta\Psi$m is a key step in the mitochondrial apoptotic pathway (23). Thus, to further validate the efficiency of andrographolide to disrupt the $\Delta\Psi$m in HT-29 cells, we used mitochondria specific, cationic, voltage-dependent green fluorochrome rhodamine123 (Rh123). Disruption of mitochondrial potential has been shown to be featured with the decrease in Rh123 retention and fluorescence. As shown in the photomicrographs, the fluorescence intensity of Rh123 decreased with the increased dose of andrographolide (16, 32, 64, 128, and 256 μM), indicating disruption of $\Delta\Psi$m (Fig. 8A). Thus, the results showed that andrographolide reduced the $\Delta\Psi$m in a dose-dependent manner.

Furthermore, the mitochondrial membrane depolarization in HT-29 cells, upon andrographolide treatment, was also confirmed with Mitotracker Red CMX Ros. The dye bounds to mitochondria of the living cells utilizing the mitochondrial potential and remains bound to the mitochondria even the cells are fixed or dead (24). As shown in the photomicrographs, the results were in agreement with the Rh123 staining and a decrease in the

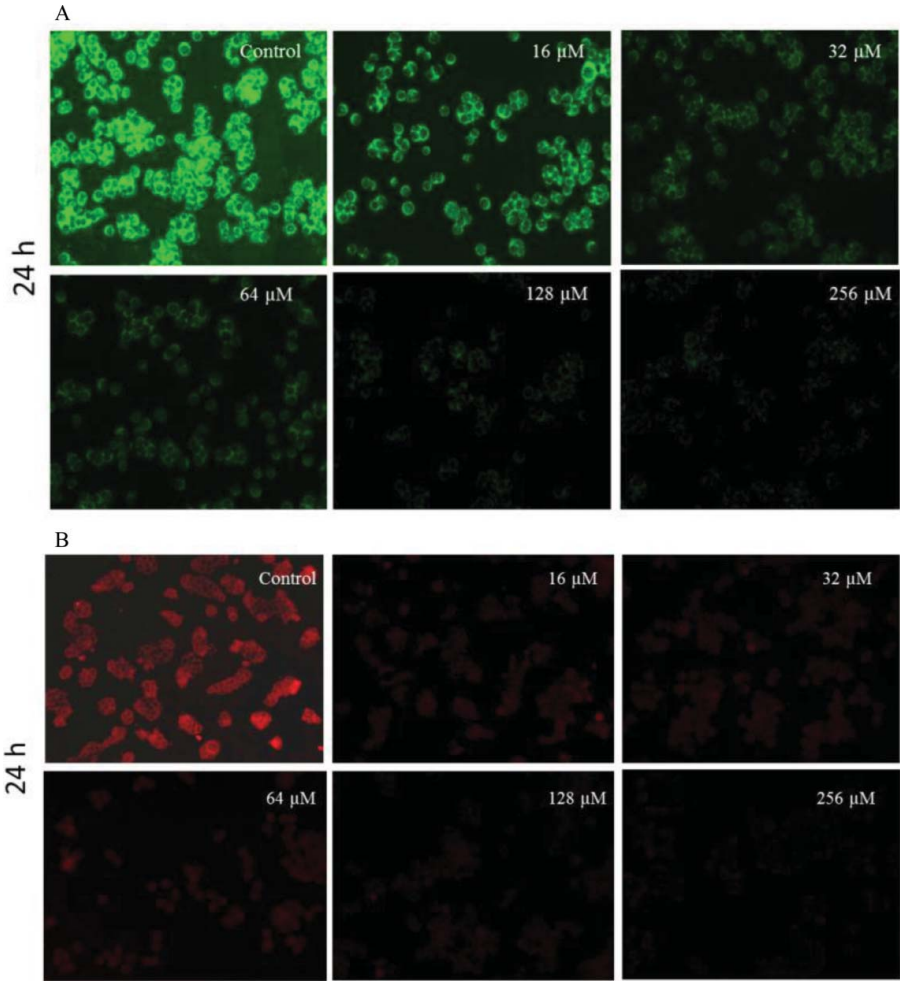

Figure 8. Mitochondrial depolarization in andrographolide treated HT-29 cells. A: Disruption of the mitochondrial membrane potential ($\Delta\Psi m$) of HT-29 cells treated with andrographolide (16–256 μM) and observed by staining with a fluorescent dye Rh123. B: Mito tracker Red CMXROS. Figures shown are representative of three independent experiments.

intensity of the Mitotracker Red CMX Ros was observed indicating the disruption of the $\Delta\Psi m$ with the increase in the dose of andrographolide (16, 32, 64, 128, and 256 μM) in a dose-dependent manner (Fig. 8B).

Andrographolide-Augmented Intracellular ROS Generation in HT-29 Cells

To elucidate the mechanism of action of andrographolide, we further investigated the effect of andrographolide on the intracellular redox status in colon cancer cells. Dysregulation of cellular redox mechanism is known to activate caspase-independent and caspase-dependent forms of cell death (25). An increased intracellular ROS generation has been reported to be associated with the initiation of apoptosis (26). Thus, we implemented H_2DCFDA fluorescent staining method to evaluate variation in intracellular ROS generation in andrographolide-treated and andrographolide-untreated colon cancer cells. Briefly, H_2DCFDA staining was applied to HT-29 cells to detect the changes in intracellular ROS level after 12 h of andrographolide (16, 32, 64, 128, and 256 μM) treatment. The fluorescent micrographs depicted that andrographolide augmented ROS generation in HT-29 cells in a dose-dependent manner (Fig. 9A). As compared to untreated control cells, andrographolide treatment resulted in enhanced fluorescence intensity in HT-29 cells, which indicated an increased intracellular ROS level. Our above finding was further confirmed by the quantitative measurement of intracellular ROS level which showed that 16 μM of andrographolide increased ROS level in HT-29 cells by around 19.81% as compared to control; which was further augmented to approximately 32.09%, 51.56%, 78.19%, and 197.23% when the dose of andrographolide was increased to 32, 64, 128, and 256 μM, respectively (Fig. 9B). Moreover, to substantiate the andrographolide-mediated increase of ROS generation, quantitative estimation of intracellular ROS

level was performed in colon cancer HT-29 cells pre-treated with a known ROS inhibitor, NAC (10 mM), followed by andrographolide (16, 32, 64, 128, and 256 μM). The results showed that pretreatment of NAC attenuated the increased ROS level in andrographolide-treated cells which corroborated our finding that andrographolide could enhance ROS generation in cancer cells (Fig. 9C).

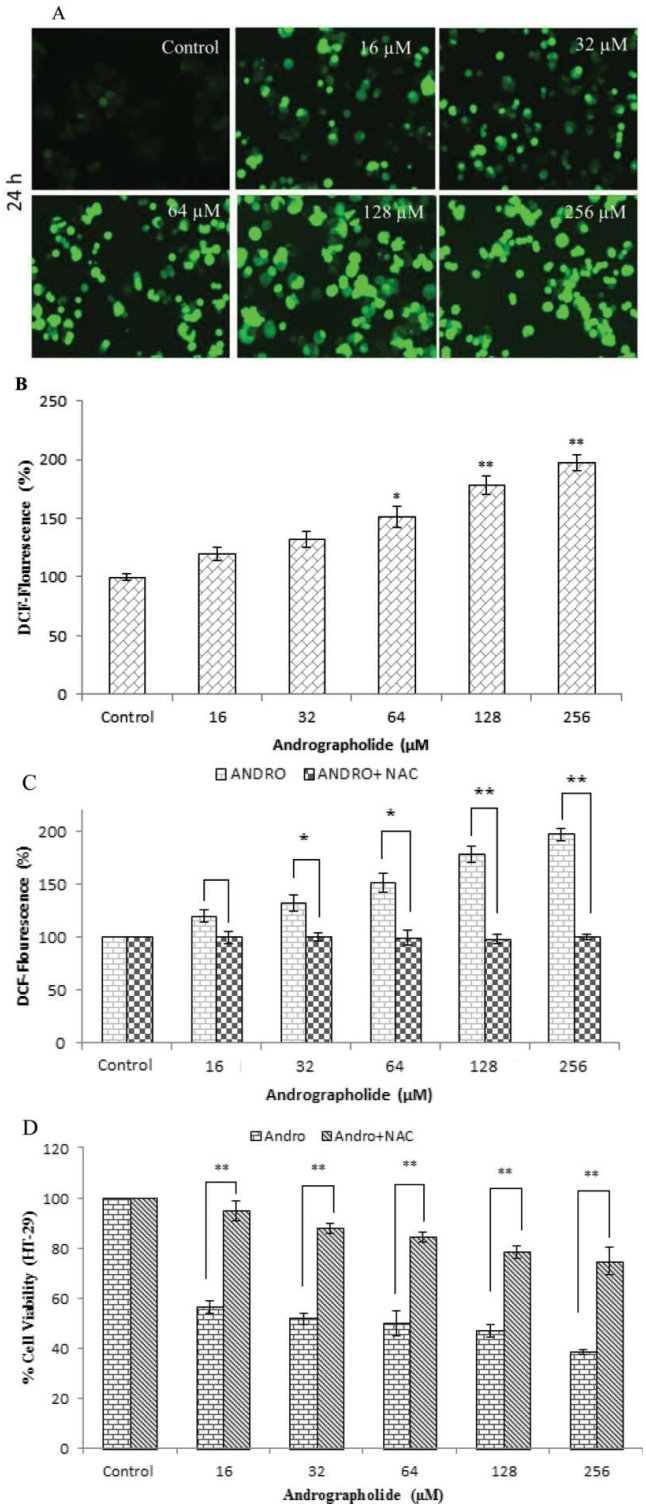

Attenuation of Andrographolide-Induced Cytotoxicity in HT-29 Cells by N-Acetyl-L-Cysteine (NAC)

To further analyze whether andrographolide-induced cytotoxicity in colon cancer cells was due to augmented ROS generation, we investigated the effect of andrographolide in HT-29 cells in the presence of NAC by MTT assay. Briefly, HT-29 cells were treated with the ROS scavenger NAC (10 mM) for 2 h followed by andrographolide (16, 32, 64, 128, and 256 μM) for an additional 24 h. The results showed that pretreatment with ROS inhibitor, NAC, significantly reduced the amount of cytotoxicity in colon cancer cells induced by andrographolide as depicted in Fig. 9D. These data indicated the critical role of augmented intracellular ROS production in andrographolide-induced apoptosis. However, pretreatment of NAC did not completely inhibit the cell viability in colon cancer cells; it indicated the involvement of other pathways also in the execution of program cell death in andrographolide-treated HT-29 cells.

Andrographolide-Induced Cell Cycle Arrest in HT-29 Cells

To determine whether suppression of colon cancer cell proliferation by andrographolide resulted from disruption of cell cycle progression, distribution of cells in different phases of the cell cycle was measured by a flow cytometer. Briefly, HT-29 cells were treated with 16, 32, 64, 128, and 256 μM andrographolide for 24 h followed by PI staining and subjected to flow cytometry analysis. The result showed that andrographolide treatment over 24 h caused a significant cell cycle arrest in HT-29 cells at G_2/M phase (Fig. 10A & B). Colon cancer cells in untreated control were found to be 64.54%, 10.84%, and 24.61% in G_0/G_1, G_2/M, and S phase, respectively.

Figure 9. Intracellular ROS generation in HT-29 cells treated with andrographolide. A: Enhanced ROS generation in DCFH-DA stained HT-29 cells treated with different concentrations of andrographolide (16–256 μM) analyzed by fluorescence microscopy. Data shown are representative of three independent experiments. B: Quantification of ROS level in terms of percent DCFDA fluorescence in HT-29 cells treated with different concentrations of andrographolide (16–256 μM). C: ROS level in HT-29 cells pre-treated with a ROS inhibitor, NAC (10 mM) followed by different doses of andrographolide (16–256 μM). D: Percent cell viability of HT-29 cells pre-treated with NAC (10 mM) followed by different doses of andrographolide (16–256 μM) for 24 h assessed by MTT assay. Values are expressed as mean ± SEM of three independent experiments performed in triplicate ($^{**}P <$ 0.01 and $^{**}P < 0.001$ as compared with control).

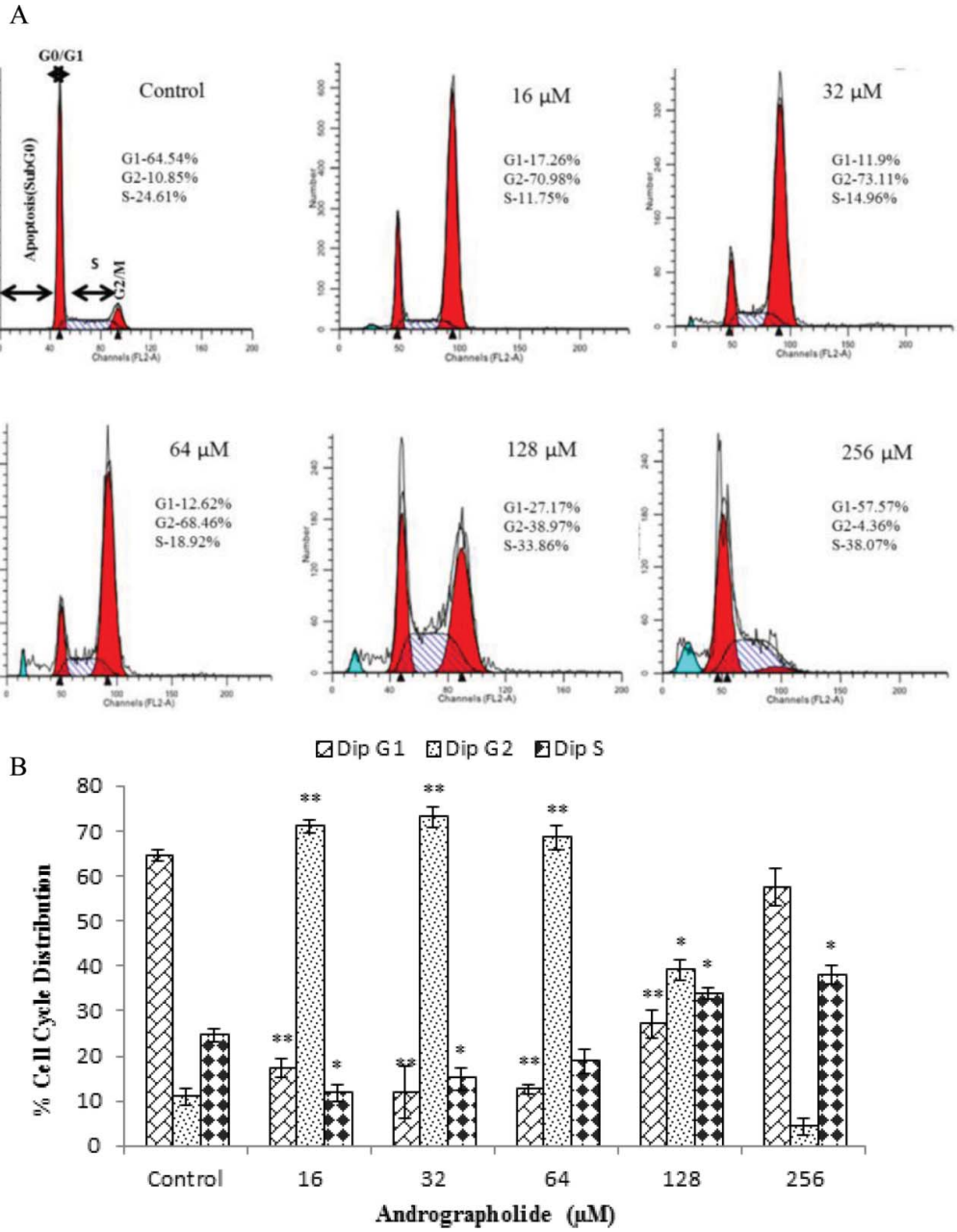

Figure 10. Andrographolide-induced cell cycle arrest in HT-29 cells. A: Cell cycle distribution of propidium iodide-stained HT-29 cells treated with andrographolide (16–256 μM) for 24 h observed by flow cytometric analysis. Data shown are representative of three independent experiments. B: Graphical representation of percent cell cycle distribution as determined by flow cytometric analysis. Data represent mean ± SEM of three independent experiments performed in triplicate ($^{*}P < 0.01$ and $^{**}P < 0.001$ as compared to control).

Andrographolide treatment of colon cancer cells with 16 μM resulted in marked reduction of S (11.75%) and G_0/G_1 (17.26%) phase cell population and increase in G_2/M (70.98%) phase population (Fig. 10A). An additional increase in the dose of andrographolide to 32 μM exhibited a more prominent reduction of cells in G_0/G_1 phase (11.90%) with a concomitant increase of cells in G_2/M phase (73.11%) (Fig. 10B). Interestingly, when the dose was increased to 64, 128, and 256 μM, G_2/M phase cell population was markedly decreased to 68.46%, 38.97%, and 4.36%, respectively, while G_0/G_1 phase population was significantly increased to 12.62%, 27.17%, and 57.57% at the respective doses (Fig. 10B). Thus, the intriguing results suggested that andrographolide induced cell cycle arrest initially in G_2/M phase at lower concentrations and this arrest was shifted to G_0/G_1 phase

at higher dose. This interesting phenomenon might be associated with the inhibitory effect of andrographolide on colon cancer HT-29 cells.

Discussion

Colorectal cancer is the leading cause of cancer-related deaths worldwide. First line treatment for colorectal cancer in early stages is surgical removal, whereas advanced stage patients are targeted with combination chemotherapy (27). However, the side effects like nephrotoxicity, hepatotoxicity, diarrhea, decreased blood count, nausea, nerve damage, fatigue, and pain are accompanied with the chemotherapy (28). For these reasons, the naturally occurring purified plant compounds are gaining great attention in current cancer research due to their antitumor, antiangiogenic, and antimetastatic properties without any significant side effects. Andrographolide, major constituent of *A. paniculata*, has been implicated in various pharmacological properties. Recent studies have suggested its ability to inhibit cancer cell proliferation, promote apoptosis, and induce cell cycle arrest in several human cancers (15,29). However, the effect of andrographolide on colon cancer has not been completely explored yet. Thus, in this study we investigated the inhibitory property of andrographolide against colon cancer cells to validate its potential as a possible anticancer agent against colorectal cancer.

In the current study, we systematically determined the antiproliferative property and possible mode of action of andrographolide against colon cancer HT-29 cells. The results of MTT assay and trypan blue exclusion assay suggested that andrographolide significantly decreased the cell viability of colon cancer HT-29 cells in a dose- and time-dependent pattern. Moreover, the morphological analysis through phase contrast microscopy of treated cells showed notable variations like detached cells and cellular shrinkage. We also assessed the cytotoxicity of andrographolide on colony-forming ability of HT-29 cells which supported the previous cell viability assay results, confirming the cytotoxic potential of andrographolide against HT-29 cells. Results from previous studies have shown similar effects of andrographolide on different cancer cells (30–32). Conventional anticancer drugs not only target neoplastic cells but are also toxic to normal cells and organs (33). Therefore, there is a need for preclinical assessment of normal tissue toxicity. Thus, we assessed cytotoxicity of andrographolide on normal colon epithelial cells, and found no toxic effect of andrographolide on colon epithelial cells. These intriguing results depict the cytotoxic potential of andrographolide against colon cancer HT-29 cells without any significant cytotoxicity on normal cells.

Apoptosis or programmed cell death is an active form of cell suicide involving concerted action of several cellular signaling pathways (23,34). Characteristic features of an apoptotic cell include membrane blebbing, cell shrinkage, chromatin condensation, and DNA fragmentation (35). Thus, we systematically investigated the characteristic feature of apoptosis induction in colon cancer cells upon treatment of andrographolide. To confirm the apoptosis-inducing effect of andrographolide, Hoechst 33342 and DAPI staining were performed which showed prominent nuclear changes like condensation and fragmentation. We further confirmed apoptosis induction in HT-29 cells, upon andrographolide treatment, by Annexin V-FITC and PI double staining. Translocation of phosphatidylserine from inner to outer leaflet of the plasma membrane is considered as an early apoptotic hallmark. Annexin V, a Ca^{2+} dependent phospholipid-binding protein, specifically binds to phosphatidylserine and thus is used for the detection of apoptosis. Result of the assay indicated a dose-dependent induction of apoptosis in colon cancer HT-29 cells. The above findings were in accordance with the previous studies which indicated that andrographolide induced apoptosis in various human cancers (15,16,36).

DNA fragmentation is also considered a hallmark of apoptosis; thus, we also examined the DNA fragmentation in HT-29 cells upon treatment of andrographolide. The apoptotic cells show a characteristic laddering pattern of nucleosomal DNA fragments and thus demonstrate a positive association between DNA fragmentation and apoptosis (37). Result of DNA fragmentation assay supported the prospect developed from previous reports and strengthened our observation of apoptosis induction by andrographolide treatment in HT-29 cell. Previous study have also reported that andrographolide induced DNA fragmentation in ovarian and breast cancer cells (38).

Caspases are cysteine aspartate proteases and remain in cytosol as inactive proenzymes. Upon apoptotic stimuli, initiator caspases (caspase-8 and caspase-9) undergo auto-catalytic activation, via cleavage at specific sites, which in turn activate executioner caspases (caspase-3 and caspase-7) (39). Caspase-3 is one of the key executioners of apoptosis and involved in the proteolytic cleavage of many cellular proteins (40). We, therefore, determined caspase-3 activity in andrographolide-treated HT-29 cells and observed significant amount of caspase-3 activation, suggesting apoptosis in colon cancer cells. Moreover, caspase-3 inhibitor substantially reduced andrographolide-induced cytotoxicity in HT-29 cells confirming caspase-3 activation during andrographolide-induced apoptosis. These results were in agreement with the earlier reports of andrographolide (31).

However, pretreatment of Z-DEVD-FMK did not completely inhibit the cell viability in colon cancer cells which indicated the possible additional role of caspase-independent pathway of apoptosis in andrographolide-treated HT-29 cells. Thus, it is plausible that andrographolide might induce apoptosis in HT-29 cells via both caspase-dependent and independent pathways. However, the role of caspase independent pathway, in the current study, remains to be evaluated.

As described in previous studies, loss of $\Delta\Psi m$ is an early marker of apoptosis (41). Thus, the qualitative evaluation of $\Delta\Psi m$ in andrographolide-treated HT-29 cells was performed by mitochondria specific, cationic fluorescent dye Rh123. Our finding suggested a dose-dependent decrease in $\Delta\Psi m$ of andrographolide-treated HT-29 cells. This result added to the apoptosis-inducing potential of andrographolide in colon cancer HT-29 cells. Similar dose-dependent effect on $\Delta\Psi m$ of Ramos cell line (Burkitt lymphoma) has been reported earlier, establishing the apoptosis-inducing ability of andrographolide via Rh123 staining (31).

The accumulation of free radical is a well-documented possible mechanism for cellular damage and cancer development (42). Excessive ROS production may cause oxidation of macromolecules and play crucial role in ageing and cell death (43). Results of qualitative and quantitative analysis of ROS generation depicted that andrographolide induced the ROS-mediated cell death in colon cancer HT-29 cells. However, the andrographolide-mediated augmentation of ROS level in colon cancer cells was significantly attenuated by NAC, a ROS inhibitor, further confirming the generation of excessive intracellular ROS due to andrographolide treatment. In addition, NAC considerably reduced the amount of cytotoxicity in HT-29 cells caused by andrographolide, suggesting the critical role of ROS in andrographolide-induced apoptosis. However, pretreatment of NAC did not completely abrogate the inhibitory effect of andrographolide on the cell viability of colon cancer cells, which indicated toward the contribution of additional ROS-independent pathway of apoptosis in andrographolide-treated HT-29 cells. Thus, it might be possible that andrographolide could induce apoptosis in colon cancer cells via both ROS-dependent and ROS-independent pathway. However, the role of ROS-independent pathway of apotosis, in the current study, remains to be investigated. Previously, andrographolide has been shown to induce apoptosis in cancer cells via ROS-mediated pathways (16,37,44).

Treatment of cytotoxic agent on cancer cells causes alterations in the cell cycle machinery and the subsequent decision of treated cancer cells "to die or not to die" results from a balance between protecting and promoting factors (16). However there is limited evidence of relationship between apoptosis and cell cycle arrest. Cell cycle regulation in vertebrates requires periodic activation and inactivation of unique protein kinase complexes consisting cyclins and cyclin-dependent kinases (Cdk). G_0/G_1 and the G_1/S phase transition involve strict association of these unique protein complexes (45). G_0/G_1 cell cycle arrest has been reported to be mediated by several inhibitory proteins like p16, p21, and p27 and G_2/M cell cycle arrest has been found to be associated with Cdk1 and Cdc25C proteins (46,47). Cell cycle progression is a strictly regulated cellular process in which G_0/G_1 and G_2/M phase are the major checkpoints and play crucial role in progression of cell cycle (48). Thus, to gain understanding of the andrographolide-induced effect on the cell cycle machinery of colon cancer HT-29 cells, we analyzed cell cycle progression by measuring DNA content via flow cytometric analysis. The results of our study indicated that andrographolide, at lower doses, induced cell cycle arrest initially in G_2/M phase; but, when the concentration was increased up to certain extent, arrest was shifted to G_0/G_1 phase. This interesting transition indicated toward an important molecular event undergoing in andrographolide-treated colon cancer cells and is currently being intensively investigated by our research group. Meanwhile, this remarkable cell cycle arrest might be associated with the inhibitory effect of andrographolide on colon cancer HT-29 cells. Anticancer activity of andrographolide, through blocking the cell cycle progression, has been previously reported in MCF-7 and HL-60 cells through G_0/G_1 arrest and in HepG2 cells via G_2/M arrest (15,29,49).

Conclusion

In conclusion, the results from the present study form a basis to conclude the antiproliferative and apoptotic potential of andrographolide against colon cancer cells. Andrographolide induced growth inhibition and apoptosis in colon cancer cells through ROS generation mediating the mitochondrial membrane depolarization, caspase activation, nuclear condensation, and DNA fragmentation. The study also showed that andrographolide induced cell cycle arrest in colon cancer cells. Intriguingly, andrographolide seems to exert its effect via multiple pathways. Thus, taken together results of our study direct toward the chemopreventive potential of andrographolide and its possible application in drug development. Although understanding the exact underlying molecular mechanisms of andrographolide-induced apoptosis and cell cycle arrest in colon cancer cells remain far from conclusive, our study provided new insights to further investigate the molecular mechanism of action of andrographolide against colon cancer.

Disclosure of Potential Conflicts of Interest

No potential conflicts of interest were disclosed.

Acknowledgments

The authors thank the management of the Integral University for providing the facilities to carry out this study. IK is greatly thankful to Maulana Azad National Fellowship (MANF), University Grants Commission (UGC), Government of India, for providing senior research fellowship (SRF). The manuscript was provided with manuscript number (IU/R&D/2017-MCN0086) by Research and Development Office, Integral University, Lucknow.

References

1. Siegel RL, Miller KD, Fedewa SA, Ahnen DJ, Meester RGS, et al.: Colorectal cancer statistics, 2017. *CA Cancer J Clin* **67**(3), 177–193, 2017.
2. Ferlay J, Soerjomataram II, Dikshit R, Eser S, and Mathers C, et al.: Cancer incidence and mortality worldwide: sources, methods and major patterns in GLOBOCAN 2012. *Int J Cancer* 2014. doi:10.1002/ijc.29210.
3. Center MM, Jemal A, and Ward E: International trends in colorectal cancer incidence rates. *Cancer Epidemiol Biomarkers Prev* **18**, 1688–1694, 2009. doi:10.1158/1055-9965.EPI-09-0090.
4. NCRP: *Three-Year Report of the Population Based Cancer Registries 2009–2011*. National Cancer Registry Programme, Indian Council of Medical Research (ICMR), Bangalore, India, 2013.
5. Norwati D, Harmy MY, Norhayati MN, and Amry AR: Colorectal cancer screening practices of primary care providers: results of a national survey in Malaysia. *Asian Pacific J Cancer Prev* **15**(6), 2901–2904, 2014. doi:10.7314/APJCP.2014.15.6.2901.
6. Rabik CA and Dolan ME: Molecular mechanisms of resistance and toxicity associated with platinating agents. *Cancer Treat Rev* **33**, 9–23, 2007. doi:10.1016/j.ctrv.2006.09.006.
7. Hosseini A and Ghorbani A: Cancer therapy with phytochemicals: evidence from clinical studies. *Avicenna J Phytomed* **5**(2), 84–97, 2015.
8. Samy RP, Thwin MM, Gopalakrishnakone P, and Ignacimuthu S: Ethnobotanical survey of folk plants for the treatment of snakebites in Southern part of Tamilnadu, India. *J. Ethnopharmacol* **115**, 302–312, 2008. doi:10.1016/j.jep.2007.10.006.
9. Hossain M, Urbi Z, Sule A, and Rahman KMH: *Andrographis paniculata* (Burm. f.) Wall. ex Nees: a review of ethnobotany, phytochemistry, and pharmacology. *Sci World J* **2014**, 274905, 2014.
10. Wasman S, Mahmood A, Chua LS, Alshawsh MA, and Hamdan S: Antioxidant and gastroprotective activities of *Andrographis paniculata* (Hempedu Bumi) in Sprague Dawley rat. *Indian J Exp Biol* **49**, 767–772, 2011.
11. Al- Bayaty FH, Abdulla MA, Hassan MIA, and Ali HM: Effect of *Andrographis paniculata* leaf extract on wound healing in rats. *Nat Prod Res* **26**, 423–429, 2012. doi:10.1080/14786419.2010.496114.
12. Xia YF, Ye BQ, Li YD, Wang JG, He XJ, et al.: Andrographolide attenuates inflammation by inhibition of NF-kappaB activation through covalent modification of reduced cysteine 62 of p50. *J. Immunol* **173**, 4207–4217, 2004. doi:10.4049/jimmunol.173.6.4207.
13. Reddy VL, Reddy SM, Ravikanth V, Krishnaiah P, and Goud TV, et al.: A new bis-andrographolide ether from *Andrographis paniculata* Nees and evaluation of anti-HIV activity. *Nat Prod Res* **19**, 223–230, 2005. doi:10.1080/14786410410001709197.
14. Varma A, Padh H, and Shrivastava N: Andrographolide: A new plant-derived antineoplastic entity on horizon. *Evid Based Complement Alternat Med* **2011**, 815390, 2011.
15. Yang S, Evens AM, Prachand S, Singh ATK, Bhalla S, et al.: Mitochondrial-Mediated apoptosis in lymphoma cells by the diterpenoid lactone andrographolide, the active component of *Andrographis paniculata*. *Clin Cancer Res* **16**(19), 4755–4768, 2010. doi:10.1158/1078-0432.CCR-10-0883.
16. Chen CC, Wu ML, Doerksen RJ, Ho CT, and Huang TC: Andrographolide induces apoptosis via down-regulation of glyoxalase 1 and HMG-CoA reductase in HL-60 cells. *J funct foods* **14**, 226–235, 2015. doi:10.1016/j.jff.2015.01.048.
17. Lee YC, Lin HH, Hsu CH, Wang CJ, Chiang TA, et al.: Inhibitory effects of andrographolide on migration and invasion in human non-small cell lung cancer A549 cells via down-regulation of PI3K/Akt signaling pathway. *Eur J Pharmacol* **632**, 23–32, 2010. doi:10.1016/j.ejphar.2010.01.009.
18. Cheng X, Xiao Y, Wang X, Wang P, Li H, et al.: Antitumor and proapoptotic activity of ethanolic extract and its various fractions from *Polytrichum commune L.ex Hedw* in L1210 cells. *J Ethnopharmacol* **143**, 49–56, 2012. doi:10.1016/j.jep.2012.05.054.
19. Johnson S, Nguyen V, and Coder D: Assessment of cell viability. *Current Protoc Cytometry* **65**, 9.2.1–9.2.26, 2013.
20. Liu B, Ordonez-Ercan D, Fan Z, Edgerton SM, Yang X, et al.: Downregulation of ErbB3 aborgates ErbB2-mediated tamoxifen resistance in breast cancer cells. *Int J Cancer* **120**, 1874–1882, 2007. doi:10.1002/ijc.22423.
21. Chen HM, Wua YC, Chia YC, Chang FR, Hsu HK, et al.: Gallic acid, a major component of *Toona sinensis* leaf extracts, contains a ROS-mediated anti-cancer activity in human prostate cancer cells. *Cancer Lett* **286**, 161–171, 2009. doi:10.1016/j.canlet.2009.05.040.
22. Fadok VA, Voelker DR, Campbell PA, Cohen J, Bratton DL, et al.: Exposure of phosphatidylserine on the surface of apoptotic lymphocytes triggers specific recognition and removal by macrophages. *J Immunol* **148**, 2207–2216, 1992.
23. Green DR and Reed JC: Mitochondria and apoptosis. *Science* **281**, 1309–1312, 1998. doi:10.1126/science.281.5381.1309.
24. Chazotte B: Labeling mitochondria with mitotracker dyes. *Cold Spring Harb Protoc* **2011**(8), 990–992, 2011.
25. Danial NN and Korsmeyer SJ: Cell death: critical control points. *Cell* **116**, 205–219, 2004. doi:10.1016/S0092-8674(04)00046-7.
26. Wenzel U, Nickel A, and Daniel H: alpha-Lipoic acid induces apoptosis in human colon cancer cells by increasing mitochondrial respiration with a concomitant O2-*-

generation. *Apoptosis* **10**(2), 359–368, 2005. doi:10.1007/s10495-005-0810-x.
27. Chung KY and Saltz LB: Adjuvant therapy of colon cancer: Current status and future directions. *Cancer J* **13**, 192–197, 2007. doi:10.1097/PPO.0b013e318074d26e.
28. Weijl N, Cleton F, and Osanto S: Free radicals and antioxidants in hemotherapy-induced toxicity. *Cancer Treat Rev* **23**, 209–240, 1997. doi:10.1016/S0305-7372(97)90012-8.
29. Satyanarayana C, Deevi DS, Rajagopalan R, Srinivas N, and Rajagopal S: DRF 3188 a novel semi-synthetic analog of andrographolide: cellular response to MCF 7 breast cancer cells. *BMC Cancer* **4**, 26–33, 2004. doi:10.1186/1471-2407-4-26.
30. Wong HC, Sagineedu SR, Lajis NH, Loke SC, and Stanslas J: Andrographolide induces cell cycle arrest and apoptosis in PC-3 prostate cancer cells. *AJPP* **5**(2), 225–233, 2011.
31. Yang S, Evens AM, Prachand S, Singh ATK, Bhalla S, et al.: Mitochondrial-mediated apoptosis in lymphoma cells by the diterpenoid lactone andrographolide, the active component of *Andrographis paniculata*. *Clin Cancer Res* **16**(19), 4755–4768, 2010. doi:10.1158/1078-0432.CCR-10-0883.
32. Yang SH, Wang SM, Syu JP, Chen Y, Wang SD, et al.: Andrographolide induces apoptosis of C6 Glioma Cells via the ERK-p53-Caspase 7-PARP pathway. *Biomed Res Int* **2014**, 312847, 2014.
33. Li W, Lam M, Choy D, Birkeland A, Sullivan ME, et al.: Human primary renal cells as a model for toxicity assessment of chemo-therapeutic drugs. *Toxicol In Vitro* **20**, 669–676, 2006. doi:10.1016/j.tiv.2005.09.016.
34. Green DR and Kroemer G: The pathophysiology of mitochondrial cell death. *Science* **305**, 626–629, 2004. doi:10.1126/science.1099320.
35. Savill J and Fadok V: Corpse clearance defines the meaning of cell death. *Nature* **407**, 784–788, 2000. doi:10.1038/35037722.
36. Manikam SD and Stanslas J: Andrographolide inhibits growth of promyelocytic leukemia cells by inducing retinoic acid receptor independent cell differentiation and apoptosis. *J Pharm Pharmacol* **61**, 78–79, 2009. doi:10.1211/jpp.61.01.0010.
37. Bortner CD, Oldenburg NBE, and Cidlowski JA: The role of DNA fragmentation in apoptosis. *Trends Cell Biol* **5**(1), 21–26, 1995. doi:10.1016/S0962-8924(00)88932-1.
38. Yunos NM, Mutalip SSM, Jauri MH, Yu JQ, and Huq F: Anti-proliferative and pro-apoptotic effects from sequenced combinations of andrographolide and cisplatin on ovarian cancer cell lines. *Anticancer Res* **33**, 4365–4372, 2013.
39. Cohen JJ: Programmed cell death in the immune system. *Adv Immunol* **50**, 55–85, 1991. doi:10.1016/S0065-2776(08)60822-6.
40. Inoue S, Browne G, Melino G, and Cohen GM: Ordering of caspases in cells undergoing apoptosis by the intrinsic pathway. *Cell Death Differ* **16**, 1053–1061, 2009. doi:10.1038/cdd.2009.29.
41. Ly JD, Grubb DR, and Lawen A: The mitochondrial membrane potential (deltapsi(m)) in apoptosis; an update. *Apoptosis* **8**, 115–128, 2003. doi:10.1023/A:1022945107762.
42. Valko M, Leibfritz D, Moncola J, Cronin MTD, Mazura M, et al.: Free radicals and antioxidants in normal physiological functions and human disease. *Int J Biochem Cell Biology* **39**, 44–84, 2007. doi:10.1016/j.biocel.2006.07.001.
43. Ott M, Gogvadze V, Orrenius S, and Zhivotovsky B: Mitochondria, oxidative stress and cell death. *Apoptosis* **12**, 913–922, 2007. doi:10.1007/s10495-007-0756-2.
44. Yang L, Wu D, Luo K, Wu S, and Wu P: Andrographolide enhances 5-fluorouracil-induced apoptosis via caspase-8-dependent mitochondrial pathway involving p53 participation in hepatocellular carcinoma (SMMC-7721) cells. *Cancer Lett* **276**, 180–188, 2009. doi:10.1016/j.canlet.2008.11.015.
45. Weinberg RA: The retinoblastoma protein and cell cycle control. *Cell* **81**, 323–330, 1995. doi:10.1016/0092-8674(95)90385-2.
46. Hall M, Bates S, and Peters G: Evidence for different modes of action of Cyclin-dependent kinase inhibitors p15 and p16 that bind to kinases p21, and p27 bind to Cyclins. *Oncogene* **11**, 1581–1588, 1995.
47. Li Y, Zhang P, Qiu F, Chen L, Miao C, et al.: Inactivation of PI3K/Akt signaling mediates proliferation inhibition and G2/M phase arrest induced by andrographolide in human glioblastoma cells. *Life Sci* **90**, 962–967, 2012. doi:10.1016/j.lfs.2012.04.044.
48. Vermeulen K, Bockstaele DRV, and Berneman ZN: The cell cycle: a review of regulation, deregulation and therapeutic targets in cancer. *Cell Prolif* **36**, 131–149, 2003. doi:10.1046/j.1365-2184.2003.00266.x.
49. Li J, Cheung HY, Zhang Z, Chan GK, and Fong WF: Andrographolide induces cell cycle arrest at G2/M phase and cell death in HepG2 cells via alteration of reactive oxygen species. *Eur J Pharmacol* **568**, 31–44, 2007. doi:10.1016/j.ejphar.2007.04.027.